



# Effects of the Coastal Uplift on the Kuroshio Ecosystem, Eastern Taiwan, the Western Boundary Current of the North Pacific Ocean

Chung-Chi Chen<sup>1,2\*</sup>, Chun-Yi Lu<sup>1</sup>, Sen Jan<sup>3\*</sup>, Chih-hao Hsieh<sup>3</sup> and Chih-Ching Chung<sup>4</sup>

<sup>1</sup> Department of Life Science, National Taiwan Normal University, Taipei, Taiwan, <sup>2</sup> College of Marine Sciences, National Dong Hwa University, Hualien, Taiwan, <sup>3</sup> Institute of Oceanography, National Taiwan University, Taipei, Taiwan, <sup>4</sup> Institute of Marine Environment and Ecology, National Taiwan Ocean University, Keelung, Taiwan

## OPEN ACCESS

### Edited by:

William Savidge,  
University of Georgia, United States

### Reviewed by:

Takeyoshi Nagai,  
Tokyo University of Marine Science  
and Technology, Japan  
Yuqiu Wei,  
Yellow Sea Fisheries Research  
Institute, Chinese Academy of Fishery  
Sciences (CAFS), China

### \*Correspondence:

Sen Jan  
senjan@ntu.edu.tw  
Chung-Chi Chen  
ccchen@ntnu.edu.tw

### Specialty section:

This article was submitted to  
Coastal Ocean Processes,  
a section of the journal  
Frontiers in Marine Science

**Received:** 16 October 2021

**Accepted:** 12 January 2022

**Published:** 17 February 2022

### Citation:

Chen C-C, Lu C-Y, Jan S,  
Hsieh C-h and Chung C-C (2022)  
Effects of the Coastal Uplift on  
the Kuroshio Ecosystem, Eastern  
Taiwan, the Western Boundary  
Current of the North Pacific Ocean.  
*Front. Mar. Sci.* 9:796187.  
doi: 10.3389/fmars.2022.796187

The Kuroshio is the western boundary current of the North Pacific Ocean. In the subtropical region of eastern Taiwan, a coastal uplift of the isotherms has occurred. To explore its impact on this oligotrophic ecosystem, hydrographic data along the transect line at 23.75°N were measured between September 2012 and September 2014. Results show that the intensity of coastal uplift was positively correlated to the flow volume transport of the Kuroshio. Significant dissolved inorganic nutrients were uplifted to the sunlit zone, especially in the onshore. For example, compared to the offshore, nitrate concentration increased 0.49 μM (or ~178%) in the upper 100 m of the onshore. The increased nutrients thereafter enhanced the growth of phytoplankton; for instance, the Chl *a* concentration increased 88.3%, compared to offshore, in the upper 100 m of the onshore. Phytoplankton community was mostly composed of picophytoplankton (<2 μm in size), which were dominated, in terms of relative abundance, by *Prochlorococcus* (83.6%), followed by *Synechococcus* (13.8%) and picoeukaryotes (2.7%). The relative abundance of *Prochlorococcus* increased from onshore toward offshore, but the trend was reversed for *Synechococcus* and picoeukaryotes, which may be affected by the coastal uplift. The results also suggest that the coastal uplift may support more energy transferred to higher trophic levels in this oligotrophic Kuroshio ecosystem.

**Keywords:** coastal uplift, dissolved inorganic nutrients, picoeukaryotes, picoplankton, *Prochlorococcus*, *Synechococcus*, the Kuroshio

## INTRODUCTION

The Kuroshio is the western boundary current in the North Pacific Ocean and is the counterpart of the Gulf Stream in the North Atlantic Ocean. It originates from the North Equatorial Current and becomes a pronounced current that crosses the Luzon Strait and flows along the east coast of Taiwan, and the shelf break of the East China Sea (ECS), before reaching the southeastern coast of Japan (Nitani, 1972). The Kuroshio is oligotrophic water with low biological productivity (Guo, 1991). However, several physical processes bring nutrient-rich subsurface Kuroshio water to the surface, such as upwelling, vertical mixing induced by typhoons, vertical nutrient flux induced by Kelvin–Helmholtz billows, strong northeast winter monsoons, and cyclonic mesoscale eddies (Hsu et al., 2010; Hung and Gong, 2011; Sukigara et al., 2014; Chen et al., 2015; Acabado et al., 2021). Primary production may therefore be enhanced by this uplifted nutrient-rich subsurface Kuroshio

water. These subsurface nutrients uplift processes are, however, local (e.g., upwelling in northeast Taiwan) and/or episodic and seasonal dependent events; thereafter, their impact on ecosystems may be confined spatiotemporally (e.g., Chen et al., 2015).

Another process, turbulent vertical mixing, has also been reported for the diffusion of subsurface nutrients to the sunlit layer in shelf slope along the Kuroshio (Nagai et al., 2019). Interestingly, the subsurface water uplift to shallow water has been observed on the east coast of Taiwan along Kuroshio's path (Chen et al., 2017). This suggests that its impact is in the broadened geographic range of this narrow-shelf subtropical Kuroshio ecosystem along the east coast of Taiwan. This coastal uplift effect on this oligotrophic ecosystem is, however, rarely being evaluated, especially on its biogeochemical responses (e.g., dissolved inorganic nutrient dynamics, biological production, phytoplankton composition. . .) on the shore side of the Kuroshio (Lai et al., 2021).

In the oligotrophic subtropical northwest Pacific, primary productivity is mainly contributed by the most abundant phytoplankton, e.g., *Prochlorococcus* and *Synechococcus* (Buitenhuis et al., 2012; Endo and Suzuki, 2019). During the uplift, the cold and nutrient-rich deep waters shoal to shallow water and enhance phytoplankton growth (Rochford, 1984; Roughan and Middleton, 2002). The shoaled nutrient-rich waters may be important for biological production and plankton dynamics (e.g., picoplankton composition) in oligotrophic ecosystems, such as the Kuroshio (Kobari et al., 2020; Lai et al., 2021). Using temperature modulated dilution experiments, Liu et al. (2020) have demonstrated that nutrient-dependent temperature sensitivities of picophytoplankton in the subtropical Kuroshio, one of the warmest regions of the global ocean (Wu et al., 2012); It suggests the importance of nutrient availability in evaluating the response of primary productivity to the projected ocean warming, especially in the oligotrophic ocean. The coastal uplift along the subtropical Kuroshio, off the east coast of Taiwan may therefore provide as a suitable nature ecosystem to examine those assumptions.

In addition, as stated above, the impact of the coastal uplift is rarely evaluated in the Kuroshio ecosystem, not even to elucidate the potential forces for the coastal uplift in this system. In this study, we therefore intend to reveal the potential mechanism for the causes of uplifting and its impact on the Kuroshio ecosystem, including the dynamics of nutrient and picoplankton, especially at the eastern coast of Taiwan.

## MATERIALS AND METHODS

### Study Area and Sampling

To understand the coastal uplift effect on the Kuroshio ecosystem, eight stations (K101–K108) along a transect (KTV1) between 121.72° and 123° E at 23.75° N were repeatedly surveyed across the Kuroshio, east of Taiwan (Figure 1). Samples were collected from six shipboard measurements taken from the R/V *Ocean Researcher I* between September of 2012 and 2014: September and November 2012, June and September 2013, and July and September 2014 (Table 1). At each station, seawater was sampled at eight depths (2–5, 10, 30, 50, 100, 150, 200,

and 250 m), using Teflon-coated Go-Flo bottles (20 l, General Oceanics Inc., Miami, FL, United States) mounted on a General Oceanic rosette assembly. Sub-samples were taken for analyses of dissolved inorganic nutrients [e.g., nitrate ( $\text{NO}_3^-$ ; N), phosphate ( $\text{PO}_4^{3-}$ ; P), and silicate ( $\text{SiO}_3^{2-}$ )], chlorophyll *a* (Chl *a*), autotrophic picoplankton (e.g., *Synechococcus*, *Prochlorococcus*, and picoeukaryotes), and heterotrophic bacteria (Bact), as described below. Please refer to Chen et al. (2017, 2021) for a detailed description of the methods used to collect the hydrographic data and analyze the aforementioned response variables. For reference, additional temperature profiles up- and downstream of the KTV1 transect along the Kuroshio were also measured in September 2013 and March 2006, respectively (Figure 1).

### Physical, Chemical Hydrographics, and Uplift Magnitude

Temperature and salinity were recorded to a depth of 250 m in the water column using a SeaBird CTD (SBE 9/11 puls, SBE Inc., Barre, VT, United States). Photosynthetically active radiation (PAR) was also measured to a depth of 250 m in the water column using an irradiance sensor (4 $\pi$ ; QSP-200L). The depth of the euphotic zone ( $Z_E$ ) was taken as the penetration depth of 1% of the surface light. The depth of the mixed layer ( $M_D$ ) was based on the potential density criterion of  $0.125 \text{ kg m}^{-3}$  (Levitus, 1982). To evaluate and estimate the uplift magnitude, the uplift area ( $U_A$ ) was applied to the area where the water temperature  $\leq 21^\circ\text{C}$  for the upper 100 m depth along the KTV1 transect. The gridding methods of Surfer 11 (Golden Software, Inc., Golden, CO, United States) were used for this area estimation.

The velocity was measured with a shipboard 75-kHz acoustic Doppler current profiler (ADCP) in roughly the upper 600 m along the cruise track while underway. The velocity at each station was also measured from the sea surface to near the seafloor using a pair of lowered AD comprising two 300-kHz, self-contained ADCPs with a downward-looking “master” and an upward-looking “slave.” The lowered ADCP data were processed using the velocity inversion method with the bottom tracking mode (Visbeck, 2002; Thurnherr, 2010). The water volume transport ( $Q_{250}$ ;  $S_V = 10^6 \text{ m}^3 \text{ s}^{-1}$ ) in the upper 250 m across the KTV1 was then calculated using positive normal velocities (i.e.,  $v > 0 \text{ m s}^{-1}$ ) on a grid 10-km wide by 8-m thick over the transect. Portions of the dataset assessed herein (i.e., water volume transport, temperature, salinity, and normal velocity) were published (Jan et al., 2015; Chen et al., 2017).

Water samples for dissolved inorganic nitrate, phosphate, and silicate analysis were collected from each sampling depth in 100 ml polypropylene bottles. The samples were immediately frozen in liquid nitrogen. A custom-made flow-injection analyzer was used for the nitrate, phosphate, and silicate analysis, and they were characterized by detection limits of 0.3, 0.01, and 0.5  $\mu\text{M}$ , respectively (Gong et al., 2003).

### Biological Variables and Data Analyses

The water samples (2 L) taken for Chl *a* analysis were immediately filtered through GF/F filter paper (Whatman, 47 mm) and stored in liquid nitrogen. The Chl *a* retained on the

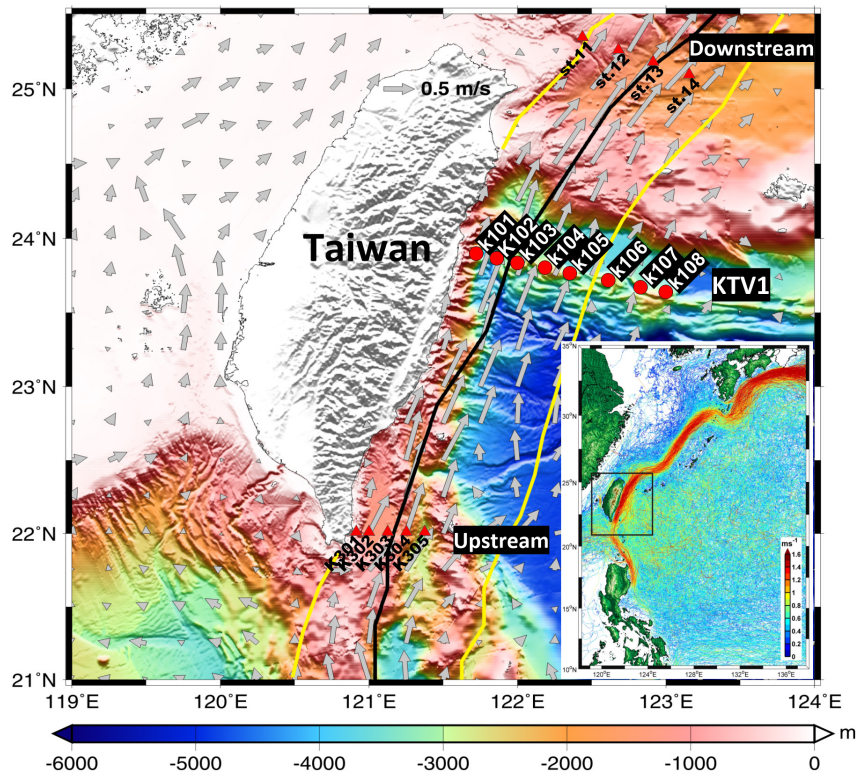


**FIGURE 1** | Sampling stations (K101–K108) along the KTV1 transect of the Kuroshio, east of Taiwan. The climatological current velocity (gray arrows) at a depth of 30 m was computed from the historical ADCP dataset available from Taiwan’s Ocean Data Bank. The bold black line indicates the maximum velocity axis at 15 m depth obtained from the surface drifter data. The solid yellow line indicates the  $0.2 \text{ m s}^{-1}$  isochron at 30 m depth obtained from the historical ADCP dataset (Jan et al., 2015). The path of the Kuroshio with velocity  $> 1 \text{ m s}^{-1}$  is indicated by surface drifter trajectories and speeds (data available at <http://www.coriolis.eu.org/Data-Products/Data-Delivery/Data-selection>) in the lower right inset where the black dotted rectangle marks the map area.

GF/F filters was quantified fluorometrically (Turner Design 10-AU-005), as in Parsons et al. (1984). When applicable, Chl *a* was converted to carbon units using a C:Chl ratio of 65.9, which was estimated from the integrated value over the upper 200 m of the Kuroshio waters (KW; Furuya, 1990).

Water samples for picoplankton enumeration were fixed in seawater-buffered paraformaldehyde at a final concentration of 0.2% (w/v) in the dark (Liu et al., 1997); they were subsequently frozen and stored in liquid nitrogen until further analysis. They were then identified and enumerated using a flow cytometer (FACSAria, Becton-Dickinson, Franklin Lakes, NJ, United States). The different picophytoplankton were distinguished based on cell size (forward- and side-scattering)

and autofluorescence in the ranges of orange from phycoerythrin ( $575 \pm 15 \text{ nm}$ , for *Synechococcus*) and red from divinyl chlorophyll ( $>670 \text{ nm}$ , for *Prochlorococcus* and photosynthetic picoeukaryotes) under excitation at 488 nm (Chan et al., 2020). The heterotrophic bacteria were stained with the nucleic acid-specific dye SYBR® Green I (emission =  $530 \pm 30 \text{ nm}$ ) in a  $10^4$ -fold-diluted commercial solution (Molecular Probes, Eugene, OR, United States; Liu et al., 2002). Known numbers of fluorescent beads (TruCOUNT Tubes, Becton-Dickinson, Franklin Lakes, NJ, United States) were simultaneously used as an instrument internal standard (Chung and Gong, 2019; Chan et al., 2020). When applicable, cell abundances were converted to carbon units using the factors widely applied, including  $53 \text{ fg C cell}^{-1}$  for *Prochlorococcus*,  $250 \text{ fg C cell}^{-1}$  for *Synechococcus*,  $2100 \text{ fg C cell}^{-1}$  for picoeukaryotes, and  $20 \text{ fg C cell}^{-1}$  for heterotrophic bacteria (Lee and Fuhrman, 1987; Morel et al., 1993; Campbell et al., 1994; Buck et al., 1996).

For comparison, the depth-integrated value of chemical and biological variables for the upper 100 m (down to the photic layer depth; see below for details) water depth were estimated using the trapezoidal method for each station. The mean depth-integrated value of variables was averaged over all stations of the KTV1 transect for each sampling period. The depth-integrated and its mean values were applied for further comparison and

**TABLE 1** | The estimated coastal uplift area ( $U_A$ ;  $\text{km}^2$ ), water volume transport ( $Q_{250}$ ;  $S_V = 10^6 \text{ m}^3 \text{ s}^{-1}$ ) in the upper 250 m of water depth at different sampling periods.

Date	2012/09	2012/11	2013/06	2013/09	2014/07	2014/09
$U_A$	0.0	6.2	61.6	0.2	33.0	9.5
$Q_{250}$	20.1	18.4	22.9	15.7	19.9	18.8

Please refer to the “Materials and Methods” section for a detailed estimation of the uplift area.

analysis. SigmaStat (ver. 3.5, Systat Software, Inc., Chicago, IL, United States) was used for simple and multiple linear regression analyses and for analysis of variance (ANOVA).

## RESULTS

### Physical and Chemical Hydrographics in the Kuroshio

#### Physical Hydrographic

In the Kuroshio, east of Taiwan, high surface temperature and salinity were observed with the mean values  $\pm$  standard deviation (SD; for this and all parameters discussed henceforth) in the range of 26.1 ( $\pm$  0.2)–30.2 ( $\pm$  0.8) $^{\circ}$ C and 33.77 ( $\pm$  0.17)–34.37 ( $\pm$  0.32) over each sampling period, respectively. Vertically, seawater temperature displayed a coastal uplift (i.e., onshore uplifting and offshore deepening) of the isotherms along the KTV1 transect using data from July 2014 as a typical example (**Figure 2a**). As for the  $M_D$  depth, it was shallower in the summer and deeper in other seasons, and its average value over each sampling period ranged from 12.9 ( $\pm$  3.9) to 72.4 ( $\pm$  25.6) m. The  $Z_E$  was however more consistent with an average depth of 103.2 ( $\pm$  12.3) m.

To evaluate the coastal uplift magnitude, the uplift area is estimated and serves as an index (see methods for details), and its area ranged from 0.0 to 61.6 km<sup>2</sup> at different sampling periods (**Table 1**). Interestingly, the uplift area was linear, in the significant margin, related to the water volume transport ( $Q_{250}$ ; **Figure 3**). The mean values of  $Q_{250}$  over each sampling period were in the range of 15.7–22.9  $S_V$  (**Table 1**). Additionally, the coastal uplift phenomenon was not only observed in the KTV1 transect; it was also found in its upstream and downstream (**Supplementary Figure S1**).

#### Chemical Hydrographic

In the oligotrophic Kuroshio, the nutrient concentrations in the surface water were not as low as expected; for example, its nitrate and phosphate values were 0.69  $\mu$ M (St. K103) and 0.08  $\mu$ M (St. K102), respectively, in July 2014 (**Figures 2b,c**). This phenomenon was also observed at other sampling periods. On average, the values for nitrate, phosphate, and silicate in the surface water were in the range of 0.00 ( $\pm$  0.00)–0.28 ( $\pm$  0.23)  $\mu$ M, 0.02 ( $\pm$  0.00)–0.10 ( $\pm$  0.02)  $\mu$ M, and 0.44 ( $\pm$  0.22)–3.19 ( $\pm$  1.30)  $\mu$ M over each sampling period, respectively. The mean depth-integrated (i.e., the upper 100 m water depth) nutrient concentrations were in the range of 0.22 ( $\pm$  0.28)–2.06 ( $\pm$  0.89)  $\mu$ M for nitrate, 0.05 ( $\pm$  0.02)–0.21 ( $\pm$  0.04)  $\mu$ M for phosphate, and 0.32 ( $\pm$  0.15)–4.68 ( $\pm$  1.08)  $\mu$ M for silicate over each sampling period. Additionally, the molar ratio of nitrate to phosphate (the N/P ratio) was in the range of 9.6–29.5 over each sampling period, with an average value of 10.4 (**Supplementary Figure S2**). Corresponding to the isotherms uplifting, nutrient concentrations (i.e., nitrate and phosphate) also demonstrated a coastal uplift pattern along the KTV1 transect (**Figures 2a–c**). For example, both nitrate ( $\geq$  1.0  $\mu$ M) and phosphate ( $\geq$  0.1  $\mu$ M) concentration contours could shoal to 30 m in the onshore stations; however, this depth could deepen to 150 and 250 m in the offshore stations (**Figures 2b,c**). A positive

linear relationship was also significantly evidenced between the mean depth-integrated nitrate (or phosphate) concentration and the uplift area over each sampling period (all  $p < 0.05$ ; **Figure 4a**), but not for silicate. The coastal uplift trend was also observed but not statistically significant between the uplift area vs. the difference between the average depth-integrated nitrate value of onshore Sts. (K101–104), and offshore, Sts. (K105–108) stations over each sampling period ( $p = 0.06$ ; **Figure 5a**).

### Biological Variables in the Kuroshio

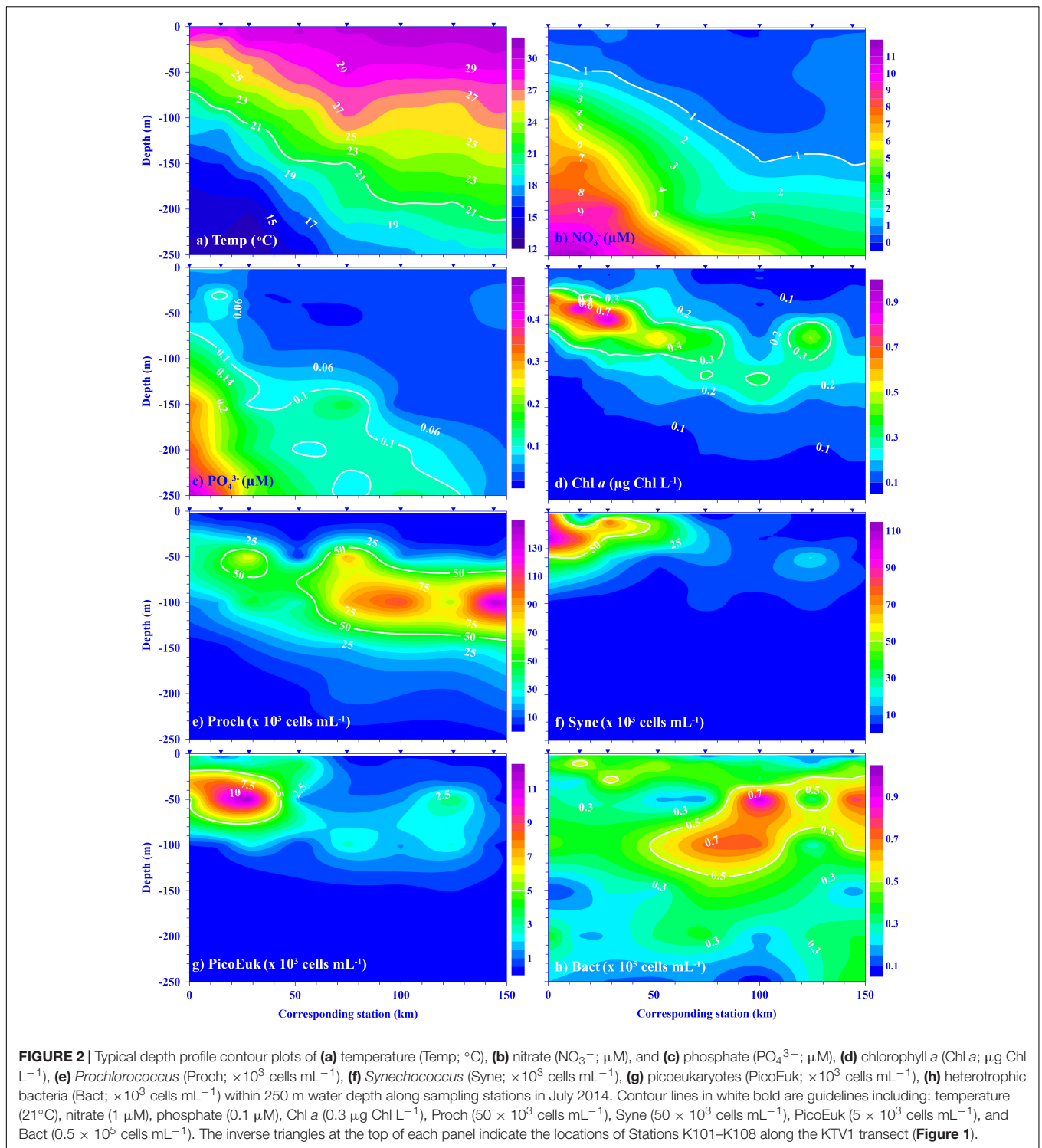
#### Chl *a* Distribution

In this oligotrophic Kuroshio ecosystem, the mean Chl *a* concentration in the surface water ranged from 0.07 ( $\pm$  0.03) to 0.33 ( $\pm$  0.25)  $\mu$ g Chl L<sup>-1</sup> over each sampling period. The mean depth-integrated Chl *a* value was in the range of 0.19 ( $\pm$  0.05) to 0.49 ( $\pm$  0.23)  $\mu$ g Chl L<sup>-1</sup> over each sampling period. Furthermore, a significant linear relationship was evidenced between the depth-integrated values of Chl *a* and nutrients (e.g., nitrate, phosphate, or silicate) using all pooled data over each sampling station (all  $p < 0.01$ ; **Table 2**).

The spatial and vertical distributions of Chl *a* may represent a variable response to nutrient uplifting impact on the Kuroshio ecosystem. The coastal uplift was also observed in the Chl *a* distribution pattern; for example, its value at the subsurface Chl *a* maximum (SCM) was higher and located shallower in the onshore compared to that of offshore in the KTV1 (**Figure 2d**). A similar coastal uplift pattern was also demonstrated in other sampling periods, and the SCM with a value could reach 2.03  $\mu$ g Chl L<sup>-1</sup> located at 30 m water depth in June 2013 (**Supplementary Figure S3**). A significant linear relationship was also evidenced between the uplift area and the mean depth-integrated Chl *a* concentration over each sampling period ( $p < 0.05$ ; **Figure 4b**). The difference between the average depth-integrated Chl *a* value of onshore (Sts. K101–104) and offshore (Sts. K105–108) stations significantly and linearly increased with increasing of the uplift area ( $p \leq 0.01$ ; **Figure 5b**).

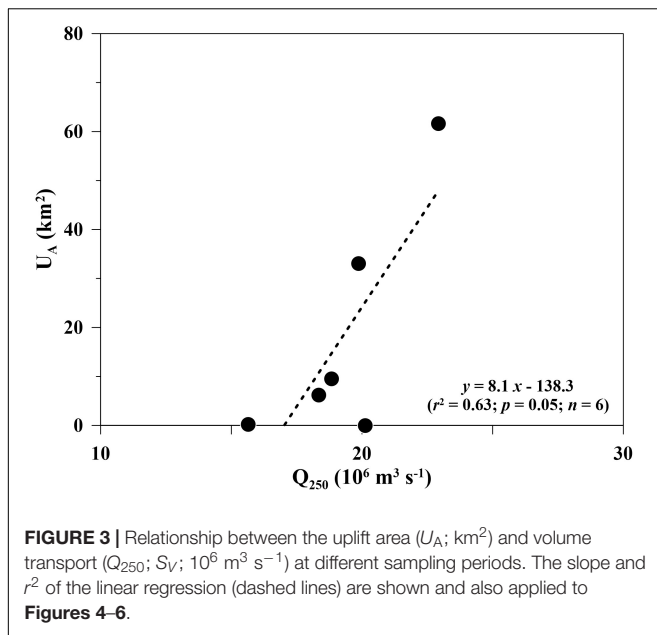
#### Picoplankton Abundance and Distribution

In this study, the Chl *a* concentration was significantly and linearly regressed with total autotrophic picoplankton abundances using the depth-integrated values for the upper 100 m depth of all sampling stations ( $p < 0.05$ ; **Figure 6a**). As for autotrophic picoplankton, it was dominated by *Prochlorococcus*, followed by *Synechococcus* and then picoeukaryotes, with an average relative abundance of 83.6 ( $\pm$  12.5)%, 13.8 ( $\pm$  11.1)%, and 2.7 ( $\pm$  1.6)%, respectively. The mean depth-integrated abundances of *Prochlorococcus*, *Synechococcus*, and picoeukaryotes were in the range of 21.34 ( $\pm$  8.62)–93.64 ( $\pm$  26.61)  $\times 10^3$  cells mL<sup>-1</sup>, 2.87 ( $\pm$  1.71)–21.51 ( $\pm$  18.22)  $\times 10^3$  cells mL<sup>-1</sup>, and 0.80 ( $\pm$  0.55)–2.89 ( $\pm$  2.28)  $\times 10^3$  cells mL<sup>-1</sup> over each sampling period, respectively (**Figure 7**); its biomass was in the range of 1.13 ( $\pm$  0.46)–4.96 ( $\pm$  1.14)  $\mu$ g C L<sup>-1</sup>, 0.72 ( $\pm$  0.43)–5.38 ( $\pm$  4.56)  $\mu$ g C L<sup>-1</sup>, and 1.68 ( $\pm$  1.15)–6.08 ( $\pm$  4.79)  $\mu$ g C L<sup>-1</sup>, respectively. The depth-integrated abundance of autotrophic picoplankton was significantly related to the depth-integrated nutrient concentration (e.g., nitrate, phosphate, or silicate), in most cases, with negative slope for *Prochlorococcus* and positive



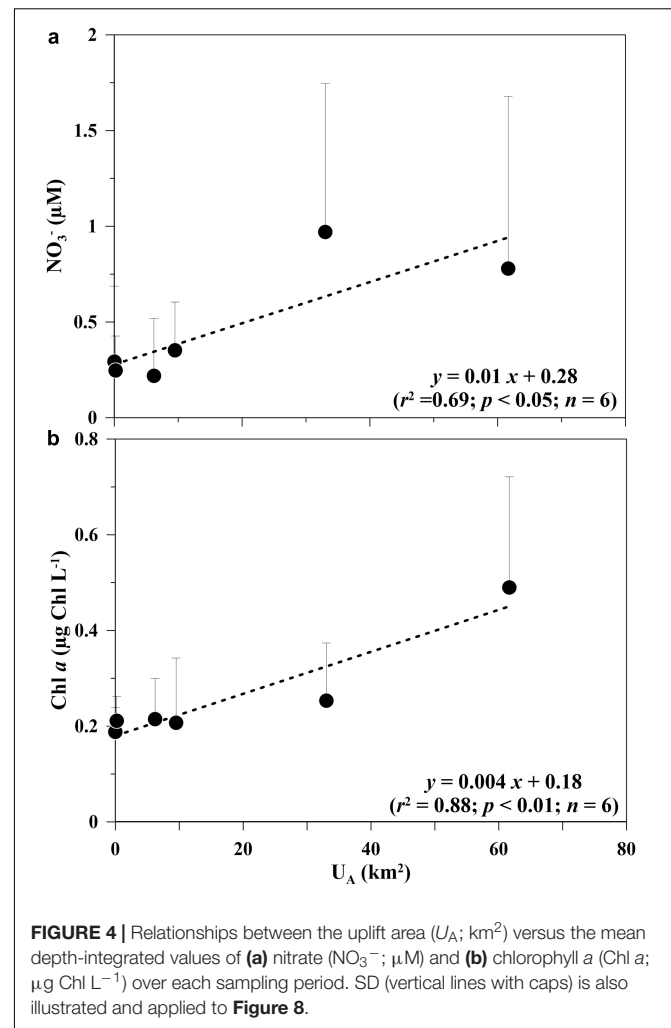
slope for *Synechococcus* and picoeukaryotes using all pooled data at each sampling station (**Table 2**); the linear relationships were also significantly evidenced for the N/P ratio (all  $p < 0.001$ ; **Table 2**). The relative abundance of autotrophic picoplankton to total autotrophic picoplankton was significantly and linearly regressed with the N/P ratio, but not for nutrient concentrations,

for values over each sampling period (**Supplementary Figure S4**); its slope was negative for *Prochlorococcus* ( $p < 0.01$ ) but positive for *Synechococcus* ( $p < 0.01$ ) and picoeukaryotes ( $p < 0.05$ ; **Supplementary Figure S4**). The result also indicates that abundances of *Prochlorococcus* decreased, but *Synechococcus* and picoeukaryotes increased with increasing of the N/P ratio or



nitrate concentration. This phenomenon could also be evidenced in the spatial, both vertical and horizontal, distribution of autotrophic picoplankton. Generally, the abundances of *Synechococcus* and picoeukaryotes were higher in the shallow water at onshore stations (**Figures 2f,g**), but a higher abundance of *Prochlorococcus* was observed in the deeper water at offshore stations (**Figure 2e**). The relative abundance of *Prochlorococcus* increased from onshore toward offshore, ranging from 71.8 ( $\pm 18.2$ ) to 93.5 ( $\pm 3.22$ )% for the upper 100 m depth (**Figure 8**). However, the trend was inverse for *Synechococcus*; that is, its relative abundance decreased from onshore toward offshore, with a range from 23.9 ( $\pm 15.9$ ) to 5.1 ( $\pm 2.5$ )%. Even though the relative abundance was small for picoeukaryotes, it also demonstrated a trend similar to that of *Synechococcus* and with values ranging from 4.3 ( $\pm 2.8$ ) to 1.4 ( $\pm 1.3$ )% (**Figure 8**).

The abundance of heterotrophic picoplankton (e.g., heterotrophic bacteria) was approximately one to two orders of magnitude higher than autotrophic picoplankton in this study. Its mean depth-integrated abundance ranged from 0.42 ( $\pm 0.13$ ) to 4.80 ( $\pm 0.94$ )  $\times 10^5$  cells  $\text{mL}^{-1}$  or biomass is in the range of 0.84 ( $\pm 0.25$ )–9.60 ( $\pm 1.89$ )  $\mu\text{g C L}^{-1}$  over each sampling period (**Figure 7**). Generally, the spatial distribution of higher heterotrophic bacteria abundance was like that of *Prochlorococcus* (**Figures 2e,h**). The depth-integrated abundance of heterotrophic bacteria was also significantly, positively and linearly regressed with *Prochlorococcus* at all sampling stations ( $r^2 = 0.61$ ;  $p < 0.001$ ); but its relationship with *Synechococcus* abundance was negative ( $r^2 = 0.10$ ;  $p < 0.05$ ; data not shown). Its depth-integrated value was also significantly, negatively and linearly related to nutrient (nitrate and silicate) concentrations and the N/P ratio, which was similar to relationships observed between *Prochlorococcus* abundance and nutrient concentrations (**Table 2**). Additionally, a linear relationship was significantly evidenced between the depth-integrated abundances (or carbon

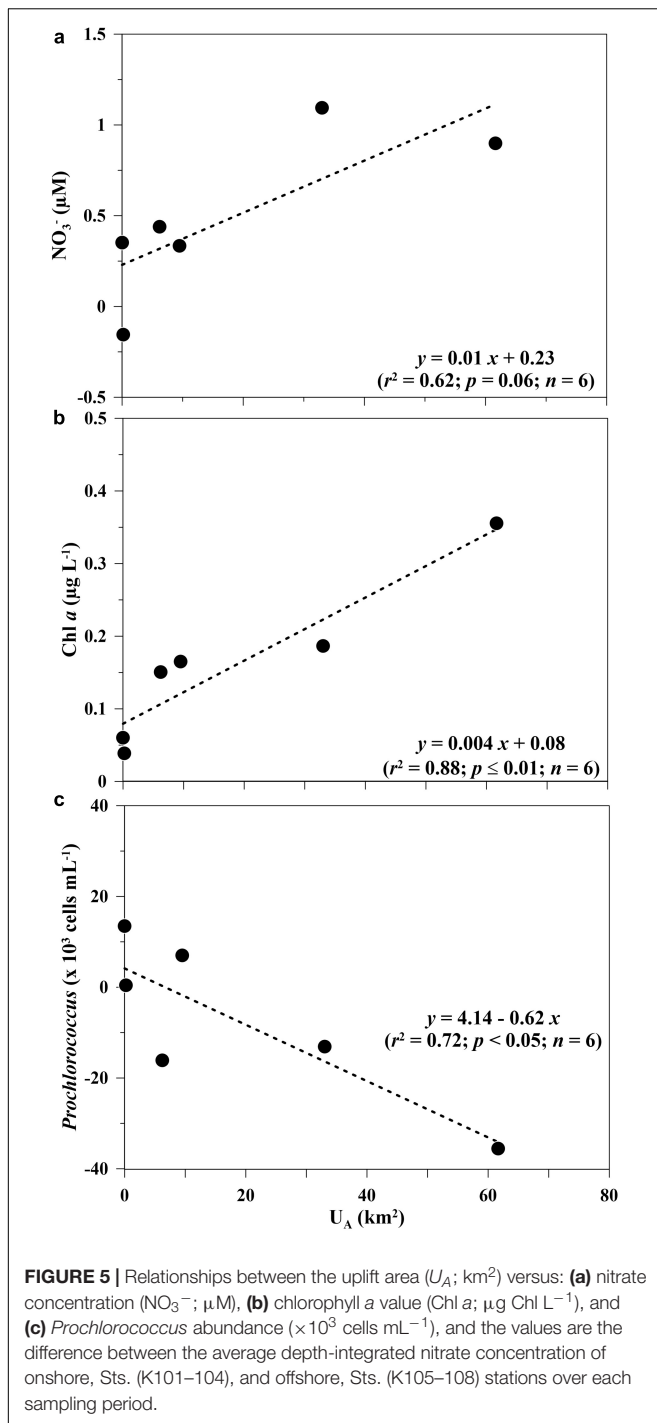


biomass) of heterotrophic bacteria and total autotrophic picoplankton using all pooled data of each sampling station ( $p < 0.001$ ; **Figure 6b**).

## DISCUSSION

### The Coastal Uplift and Its Impact on Chemical Hydrographics in the Kuroshio

The typical characteristic of KW is high salinity and high temperature, as it originates from the Northern Equatorial Current with modification from South China Sea water and West Philippine Sea water (also called North Pacific water) (Mensah et al., 2014, 2015). During its downstream transport, a tremendous amount of oligotrophic water, heat, and salt is delivered northward from its origin (Nitani, 1972). High surface temperature ( $> 26.1^\circ\text{C}$ ) and salinity ( $> 33.77$ ) were observed in this study. Vertically, seawater temperature displayed an onshore lifting and offshore deepening of the isotherms (i.e., tilting isotherms) across the Kuroshio in the KTV1 transect (**Figures 1, 2a**). This westward (shoreward)



elevated sloping isotherm (and isopycnal) is typical in the western boundary current, such as the Kuroshio, off the east coast of Taiwan (Jan et al., 2011; Chen et al., 2017). Even though this pattern is a normal characteristic of a geostrophic current, its uplifting magnitude of cold water mass, biological responses, and associated variation of these variables due to the strengthening/weakening of the geostrophic current have rarely been calculated with *in situ* data, not to mention its impact on the

**TABLE 2** | The slopes,  $r^2$  and  $p$ -values of linear regressions between the depth-integrated values of variables vs. nutrient concentrations ( $\mu\text{M}$ ) [e.g., nitrate ( $\text{NO}_3^-$ ; N), phosphate ( $\text{PO}_4^{3-}$ ; P), silicate ( $\text{SiO}_3^{2-}$ )] or the N/P molar ratio for the upper 100 m depth of all sampling stations.

Nutrients Variables	$[\text{NO}_3^-]$	$[\text{PO}_4^{3-}]$	$[\text{SiO}_3^{2-}]$	The N/P ratio
Chl <i>a</i> ( $n = 48$ )	Slope = 0.15 $r^2 = 0.41^{***}$	Slope = 1.86 $r^2 = 0.47^{***}$	Slope = 0.04 $r^2 = 0.17^{**}$	Slope = 0.01 $r^2 = 0.03$
Proch ( $n = 47$ )	Slope = -13.02 $r^2 = 0.08^*$	Slope = 110.91 $r^2 = 0.04$	Slope = -13.16 $r^2 = 0.41^{***}$	Slope = -2.46 $r^2 = 0.39^{***}$
Syne ( $n = 47$ )	Slope = 12.81 $r^2 = 0.70^{***}$	Slope = 47.90 $r^2 = 0.07$	Slope = 4.03 $r^2 = 0.34^{***}$	Slope = 1.05 $r^2 = 0.54^{***}$
PicoEuk ( $n = 47$ )	Slope = 1.59 $r^2 = 0.58^{***}$	Slope = 8.47 $r^2 = 0.12^*$	Slope = 0.57 $r^2 = 0.36^{***}$	Slope = 0.12 $r^2 = 0.40^{***}$
Bact ( $n = 47$ )	Slope = -0.69 $r^2 = 0.08^*$	Slope = 11.54 $r^2 = 0.16^{**}$	Slope = -0.80 $r^2 = 0.53^{***}$	Slope = -0.18 $r^2 = 0.65^{***}$

Variables include chlorophyll *a* (*Chl a*;  $\mu\text{g L}^{-1}$ ) concentration, abundances ( $\times 10^3$  cells  $\text{mL}^{-1}$ ) of *Prochlorococcus* (*Proch*) *Synechococcus* (*Syne*), picoeukaryotes (*PicoEuk*), as well as heterotrophic bacteria (*Bact*;  $\times 10^5$  cells  $\text{mL}^{-1}$ ).

$n$ , sampling number.

\*\*\* $p < 0.001$ ; \*\* $p < 0.01$ ; \* $p \leq 0.05$ .

ecosystem. To estimate the uplifting magnitude in the vertical, the uplift area was quantified, applied, and served as an index (see “Materials and Methods” for details; **Table 1**).

In our statistical analysis of the six cruise observations, the isotherm slope and associated uplift area on the onshore side of the Kuroshio is linearly correlated to the volume transport in the upper 250 m  $Q_{250}$  with  $r^2 = 0.63$  ( $p = 0.0059$ ; **Figure 3**). The increase of uplift area at a certain depth in the upper layer suggests the support of cold water and nutrients from lower layers, which potentially brings biological influences to the upper layer, as observed during our cruise surveys. Within the seasonal time scale (i.e., the intraseasonal time scale), the variability of the isotherm (and isopycnal) slope and associated volume transport across the Kuroshio east of Taiwan is closely related to the impingement of mesoscale eddies, which has been demonstrated and discussed using observations from moored pressure sensor-equipped inverted echo sounder (PIES) array, moored 75-kHz acoustic Doppler current profilers, ship-based hydrography surveys, and satellite altimeter data (Jan et al., 2015, 2017; Chang et al., 2018; Mensah et al., 2020). Based on the theory of geostrophic balance and the corresponding thermal wind relation of a large-scale, stratified ocean current (e.g., the Kuroshio), the increase (or decrease) of isotherm slope across the Kuroshio causes an increase (or decrease) of volume transport in the Kuroshio and vice versa (Jan et al., 2017). The thermal wind relation states a balance between geostrophic velocity shear and horizontal density gradient perpendicular to the velocity shear (e.g., Cushman-Roisin, 1994):  $\frac{\partial v_G}{\partial z} = -\frac{g}{\rho_0 f} \frac{\partial \rho}{\partial x}$  (where  $v_G$  is the northward geostrophic velocity,  $g$  is gravitational acceleration,  $\rho_0$  is reference seawater density,  $f$  is the Coriolis parameter calculated as  $2\Omega \sin$  (latitude),  $\Omega$  is the angular velocity of earth rotation, and  $\rho$  is density). As the velocity in the upper layer increases and consequently leads to the increase of the velocity shear, the density gradient is therefore adjusted to increase the isopycnal (or isotherm) slope across the current. The physical process typically causes the uplift of the isotherm/isopycnal in the onshore side of the Kuroshio, which corresponds to the increase of upward vertical velocity near the coast and consequently

creates a net nutrient flux in the vertical. As the upper layer velocity decreases, the aforementioned processes reverse. Note that the across-Kuroshio isotherm/isopycnal slope could also be influenced by the hydrography of an impinging mesoscale eddy (Jan et al., 2017). The impingement of a cyclonic eddy from the east could heave (depress) isotherms/isopycnals on the offshore (onshore) side of the Kuroshio and lead to the weakening of Kuroshio transport east of Taiwan, as illustrated in the Figure 1A of Jan et al. (2017). As an anticyclonic eddy impinges on the Kuroshio, the processes in the eddy-Kuroshio interaction reverse and the isotherm/isopycnal slope and associated Kuroshio transport increases as illustrated in the Figure 1B of Jan et al. (2017). The positive linear correlation of the onshore uplift area and  $Q_{250}$  obtained from the six of our observations can be plausibly attributed to the aforementioned dynamics. Additionally, this coastal uplift was also found in the upstream and downstream of the KTV1 transect along the Kuroshio-influenced regions (Supplementary Figure S1; Lai et al., 2021). It suggests that this coastal uplift may occur year-round in a broad-scale region on the onshore side of Kuroshio, eastern Taiwan. This also indicates that its impact on the Kuroshio ecosystem may be more profound than expected.

Despite the swift downstream advection of any variability in the Kuroshio, the frontogenesis and frontolysis occurring when mesoscale eddies of both signs impinge onto the Kuroshio and associated submesoscale processes created during the impingement (e.g., Nagai et al., 2006; McWilliams et al., 2009), particularly on the offshore side, and its potential biological influences merit a further study. Note that the mesoscale eddy influence and corresponding eddy-Kuroshio interaction is not the only cause of the uplift area and  $Q_{250}$  variability described herein. The entrainment of colder water (e.g., South China Sea water from the Luzon Strait or riverine waters from the east coast of Taiwan) to the onshore flank of the Kuroshio in the upper 200 m could also result in the change of density gradient across the Kuroshio through isotherm heaving, resulting in the increase of northward flow volume transport (Mensah et al., 2014; Jan et al., 2015). The southwesterly wind burst-induced seaward Ekman transport along the east coast and typhoons that pass across or nearby Taiwan could also contribute to the uplift of nearshore isotherms (or colder subsurface water) and the associated nutrient concentration in the upper 100–200 m, which merits a future study. It should also be noted that a decreased  $Q_{250}$  may be accompanied by the depression of isotherms on the onshore side of the upper layer Kuroshio. This downward moving process will not have a positive effect on the increase of nutrient concentration near the eastern coast of Taiwan.

Even though the KW carries oligotrophic water, the nutrient concentration is normally close to zero in the surface water (e.g., Chen et al., 1995; Kodama et al., 2014). In this study, nitrate concentration in the surface reached  $0.69 \mu\text{M}$  at St. K103, an onshore station (Figure 2b); this relatively high nutrient value in the surface water was also found at onshore stations in other sampling periods. This phenomenon might be caused by the coastal uplift. Corresponding to the isotherms coastal uplifting, nutrient distribution also demonstrated a coastal uplift pattern; that is, an onshore lifting and offshore deepening of

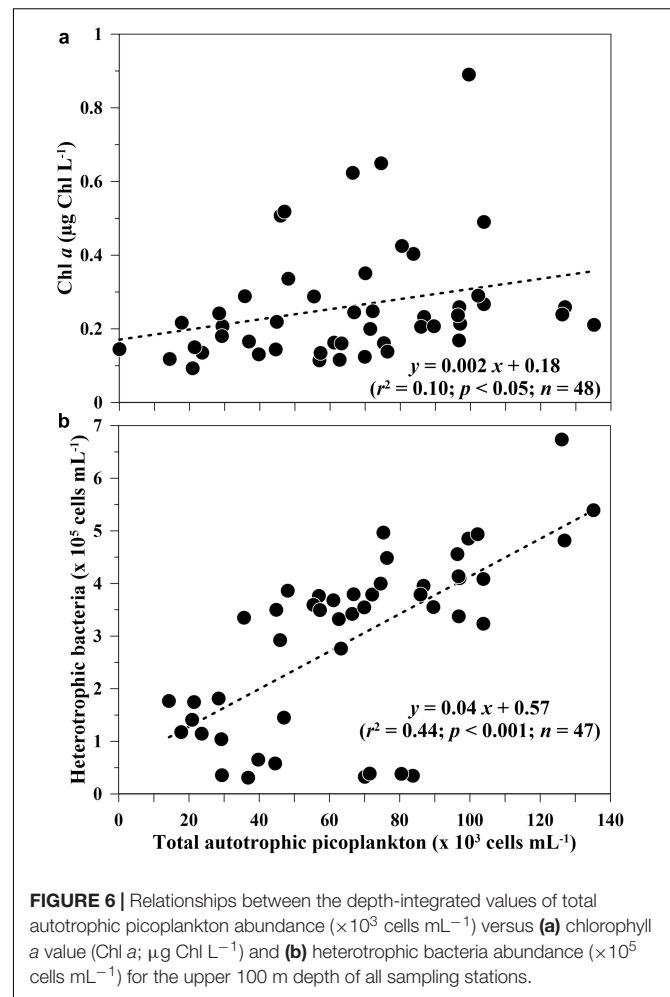


**FIGURE 6** | Relationships between the depth-integrated values of total autotrophic picoplankton abundance ( $\times 10^3$  cells  $\text{mL}^{-1}$ ) versus (a) chlorophyll a value (Chl a;  $\mu\text{g Chl L}^{-1}$ ) and (b) heterotrophic bacteria abundance ( $\times 10^5$  cells  $\text{mL}^{-1}$ ) for the upper 100 m depth of all sampling stations.

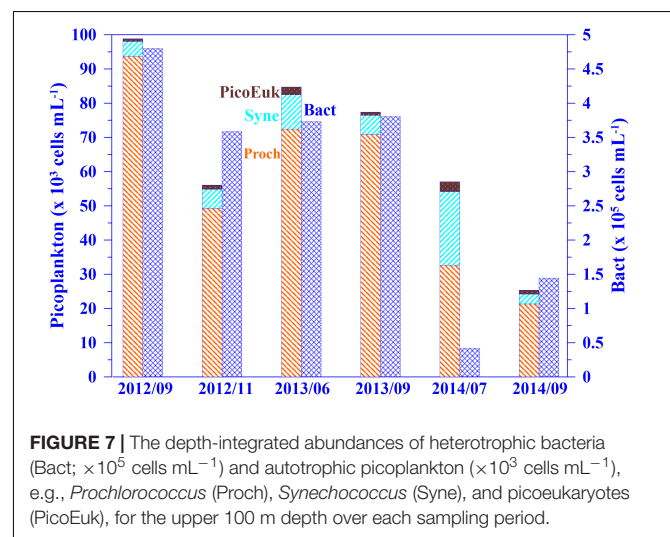
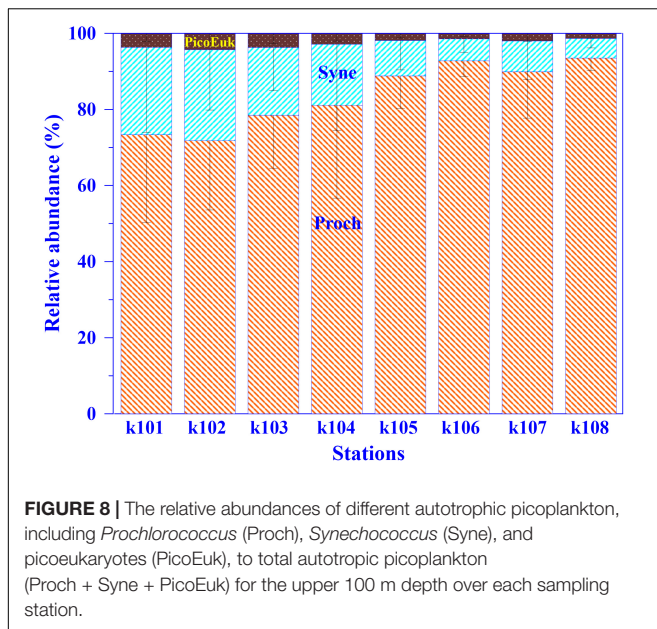


**FIGURE 7** | The depth-integrated abundances of heterotrophic bacteria (Bact;  $\times 10^5$  cells  $\text{mL}^{-1}$ ) and autotrophic picoplankton ( $\times 10^3$  cells  $\text{mL}^{-1}$ ), e.g., *Prochlorococcus* (Proch), *Synechococcus* (Syne), and picoeukaryotes (PicoEuk), for the upper 100 m depth over each sampling period.

the nutrient concentration contours along the KTV1 transect (Figures 2b,c). This pattern could be significantly evidenced by the negative linear relationships between nutrients (nitrate or phosphate) and water temperature using all pooled data in



this study; The trend was also significant for nutrients and water density but with the positive linear relationships (all  $p < 0.001$ ; data not shown). This assumption was also supported by the significant linear relationship between the nutrient concentrations and the uplift area (Figure 4a). Additionally, there was also a trend displayed that the difference of average nutrient value between onshore and offshore stations increased with increasing of the uplift magnitude, even though it was not statistically significant (Figure 5a). In addition to dissolved inorganic nutrient concentration/availability, the N/P ratio also has important implications for marine plankton (Wal et al., 1994; Agawin et al., 2004). The average N/P ratio was small, with a value of 10.4 in this study (Supplementary Figure S2). This ratio is consistent with the KW properties characterized by a low N/P ratio (e.g.,  $< 16$ ; Kodama et al., 2014). Noticeably, the N/P ratio varied spatiotemporally in this study, and this might result in variant responses on marine plankton (Supplementary Figure S2). The results all suggest that the pelagic ecosystem across the Kuroshio mainstream (e.g., onshore to offshore) may have different responses due to its horizontal and spatial nutrient distribution and/or the variant N/P ratio.

## Coastal Uplift Impact on Biological Variables in the Kuroshio

Phytoplankton growth mostly depends on nutrient availability in oligotrophic KW (Lin et al., 2020; Liu et al., 2020). Light availability might not be a limited factor for phytoplankton growth in this subtropical Kuroshio region since its  $Z_E$  consistently reached 103 m water depth in this study. The nutrient availability limitation could be indirectly supported by the significant linear relationship between the values of Chl *a* and nutrients (Table 2). The coastal uplift not only enhanced the upward nutrient concentration, but it also increased phytoplankton biomass (used Chl *a* as proxy) in the shallow

water of the Kuroshio. Generally, the SCM was located shallower onshore and became deeper toward the offshore, and its value even reached  $2.03 \mu\text{g Chl L}^{-1}$  (Figure 2d and Supplementary Figure S3). The depth-integrated Chl *a* concentration also increased with an increase in the uplift magnitude (Figure 4b). Spatially, the average Chl *a* concentration was higher in the onshore than in the offshore, and the difference between onshore and offshore stations was also significantly related to the uplift magnitude (Figure 5b). This suggests that the coastal uplift of nutrients may enhance the growth of phytoplankton in the onshore stations, and its enhancement increased with an increase in the uplift magnitude in the Kuroshio, eastern Taiwan.

Additionally, phytoplankton composition may also vary due to nutrient availability and/or the N/P ratio (Agawin et al., 2004; Mouriño-Carballido et al., 2016; Liu et al., 2020). In the oligotrophic ocean, plankton is dominated by picoplankton, which includes both autotrophic and heterotrophic picoplankton (Marañón et al., 2001; Calvo-Díaz et al., 2011). The composition of picoplankton, especially picophytoplankton, may vary with environmental factors, such as light intensity, nutrient availability, turbulent mixing, and temperature (Smayda and Reynolds, 2001; Mouriño-Carballido et al., 2016; Liu et al., 2020). The abundance of autotrophic picoplankton was dominated by *Prochlorococcus* (83.6%), followed by *Synechococcus* (13.8%) and then picoeukaryotes (2.7%) in this study. Similar dominance of picophytoplankton abundance was also observed in the Kuroshio and the subtropical northwest Pacific. There, it was mostly dominated by *Prochlorococcus* and *Synechococcus* (Jiao and Yang, 2002; Li et al., 2017; Endo and Suzuki, 2019; Liu et al., 2020). The picoeukaryotes abundance was relatively low in a similar region, and its majority was composed of Alveolata, Haptophyta, and Stramenopiles (Chan et al., 2020). The abundance of total autotrophic picoplankton (*Prochlorococcus* + *Synechococcus* + picoeukaryotes) was significantly related to the Chl *a* concentration (Figure 6a). This suggests that phytoplankton might be dominated by autotrophic picoplankton in the Kuroshio. In oceanic waters, picophytoplankton is responsible for 46–89% of the bulk Chl *a* (Jiao and Yang, 2002). This assumption could also be supported by the high proportion of carbon biomass of picophytoplankton to phytoplankton; its proportion was approximately 50.4 ( $\pm 18.2$ )% in this study. Picophytoplankton tend to dominate the phytoplankton biomass in the oligotrophic ocean, where their high surface-to-volume ratio makes them the best competitors for low nutrient concentrations (Raven, 1998; Alvain et al., 2005; Buitenhuis et al., 2012).

The relative contribution of different picophytoplankton to its composition, however, varied spatiotemporally. Spatially, the contribution of *Prochlorococcus* to total picophytoplankton abundance increased from onshore to offshore, but the pattern was inverse for *Synechococcus* and picoeukaryotes. Additionally, the difference in *Prochlorococcus* abundance between onshore and offshore decreased with an increase in the coastal uplift magnitude (Figure 5c). This suggests that the increasing nutrient concentrations caused by the coastal uplift might decrease and/or increase the growth of *Prochlorococcus* and other picophytoplankton (e.g.,

*Synechococcus* or picoeukaryotes) onshore, respectively. This assumption could be supported by the significant linear relationship between different picophytoplankton and nutrient concentrations (e.g., nitrate and silicate), which have negative and positive slopes for *Prochlorococcus* and other picophytoplankton (e.g., *Synechococcus* or picoeukaryotes), respectively (Table 2); Mouriño-Carballido et al. (2016) have also observed similar trends. The negatively linear relationship was also evidenced between phosphate concentration versus the difference between onshore and offshore stations of *Prochlorococcus* abundance over each sampling period (data not shown;  $r^2 = 0.81$ ;  $p \leq 0.01$ ). The difference in *Synechococcus* abundance between onshore and offshore stations also significantly increased with increasing nitrate concentration (data not shown;  $r^2 = 0.67$ ;  $p < 0.05$ ). Similar to previous relationships between nitrate concentrations and picophytoplankton, the regressions were also significantly evidenced between the N/P molar ratio and picophytoplankton (Table 2 and Supplementary Figure S4). Phytoplankton species composition has also been observed and shifted with the N/P molar ratio (Agawin et al., 2004).

As for heterotrophic picoplankton (or heterotrophic bacteria), it dominates the picoplankton in oligotrophic oceans, such as the Kuroshio (Figure 7; Calvo-Díaz et al., 2011). In this study, heterotrophic bacteria were positively regressed with total autotrophic picoplankton in terms of abundance and biomass (Figure 6b). On average, the ratio of autotrophic to heterotrophic picoplankton biomass in carbon units was  $1.13 \pm 0.54$  over this study if the extremely high ratio of the July 2014 data was excluded from this estimation. This ratio was at the high end of observed values (0.81–1.21) in the North Atlantic subtropical gyre (Calvo-Díaz et al., 2011). The distribution of heterotrophic bacteria was similar to that of *Prochlorococcus*, even though its abundance was one to two orders of magnitude higher than *Prochlorococcus*. This assumption could be supported by the significant relationship found between abundances of heterotrophic bacteria and *Prochlorococcus*. The relationships between heterotrophic bacteria and nutrient concentrations or the N/P ratio were also significant and similar to that of *Prochlorococcus* (Table 2). Even though an inverse pattern was observed between biomass of heterotrophic bacteria and *Prochlorococcus* in the downstream Kuroshio (Jiao and Yang, 2002). The results suggest that heterotrophic bacteria might be partially dependent on resources derived from picophytoplankton.

## Implication of the Coastal Uplift Effect on the Kuroshio Ecosystem

The coastal uplift occurred in the onshore region with approximately  $50 \times 400$  km (width  $\times$  length) along the Kuroshio, east of Taiwan (Figures 1, 2 and Supplementary Figure S1). Coastal uplift enhanced and increased nutrient concentration in the shallow water of this onshore region; the nutrient concentration also increased with the uplift magnitude increasing (Figure 4a). Compared to the offshore region, on average, nitrate concentration increased approximately  $0.49 \mu\text{M}$  over 100 m water depth (or  $0.69 \text{ g N m}^{-2}$ ) in the onshore region; the total amount of nitrate increased approximately  $1.37 \times 10^4 \text{ T}$  of N

in the onshore region along the Kuroshio. Primary production will therefore be promoted by the enhanced nutrients in the sunlit layer, approximately 100 m in the oligotrophic Kuroshio. Unfortunately, primary production was not measured in this study. Phytoplankton biomass, however, not only increased with increasing uplift magnitude: its value was higher in the onshore than that of the offshore regions for an average value of  $0.16 \mu\text{g Chl L}^{-1}$  (or  $1.06 \text{ g C m}^{-2}$ ); the total amount of phytoplankton biomass increased approximately  $2.11 \times 10^4 \text{ T}$  of C in the onshore region along the Kuroshio, east coast of Taiwan. High phytoplankton biomass can provide and transfer energy to higher trophic levels in the pelagic ecosystem of Kuroshio. This implies that the coastal uplift may play one of the key roles in resolving the “Kuroshio paradox” (Nagai, 2019).

Picoplankton is highly susceptible to environmental changes, including altering its community compositions and/or nutrition strategy to respond (Worden et al., 2015; Chung and Gong, 2019). In addition to increasing nutrient concentrations and phytoplankton biomass, the relative abundances and composition of picophytoplankton also changed due to the coastal uplift. For example, the relative abundances of *Synechococcus* and picoeukaryotes increased toward onshore but decreased for *Prochlorococcus* (Figure 8). This implied that the organic carbon content should increase and be higher in the onshore than in the offshore regions, even if similar Chl *a* concentrations are found in both regions. Growth of *Synechococcus* and picoeukaryotes is more favorable in high nutrient availability environments, such as the onshore region of the Kuroshio (Mouriño-Carballido et al., 2016; Liu et al., 2020). The growth of *Prochlorococcus* is, however, less susceptible to nutrient depletion (or availability) but more vulnerable to higher temperature (Olson et al., 1990; Liu et al., 2020). This may explain why the higher abundance of *Prochlorococcus* was normally observed at water column where water temperature  $< 30^\circ\text{C}$ , i.e., generally, at the shallow layer onshore and deeper layer offshore (Figure 2e and Supplementary Figure S5b; Jiao and Yang, 2002). The results also suggest that this phenomenon (e.g., decreasing *Prochlorococcus* abundance) should be enhanced in the Kuroshio due to water temperature increases caused by global warming. In the subtropical Kuroshio ecosystem, surface-warming rates have been suggested approximately two to three times faster than other subtropical regions in the past decades (Wu et al., 2012). This accelerated warming may subsequently change the flow velocity of the Kuroshio Current (Wu et al., 2012, 2016; Yang et al., 2016). This implies that the previously observed phenomena (e.g., the coastal uplift magnitude and its subsequent changes in nutrient dynamics and picoplankton composition) may be intensified and enhanced by future global warming.

Growth of heterotrophic bacteria may be limited by substrate supply (e.g., organic carbon) and/or temperature in the shelf region and in the Kuroshio (Jiao and Yang, 2002; Shiah et al., 2003; Lai et al., 2021). As stated above, heterotrophic bacteria were significantly related to autotrophic picoplankton. In the coastal uplift onshore region, picophytoplankton (e.g., *Synechococcus* and picoeukaryotes) with higher organic carbon content may favor the growth of heterotrophic bacteria; its abundance was averagely higher, ca.  $0.17 \times 10^5 \text{ cells mL}^{-1}$ , in the onshore than offshore regions in this study.

## CONCLUSION

The Kuroshio is oligotrophic and low productivity, but it supports a high abundance of fish population. This is called the “Kuroshio paradox.” In this study, a coastal uplift was observed in the subtropical Kuroshio, off the east coast of Taiwan. Vertically, seawater temperature displayed an onshore lifting and offshore deepening of the isotherms across the Kuroshio. This coastal uplift occurs year-round and approximately covers the area along the Kuroshio, eastern Taiwan. Interestingly, the coastal uplift intensity (or magnitude) was significantly related to the volume transport of the upper 250 m depth in the Kuroshio. Its magnitude (e.g., isotherm slope) variation could be associated with the adjustment of the pressure gradient force and the Coriolis force, which is not balanced in the cross-stream direction. A large amount of dissolved inorganic nutrients was uplifted to the sunlit zone, and it promoted primary production especially in the onshore region; in total, it is estimated to increase approximately  $1.37 \times 10^4$  T of N and  $2.11 \times 10^4$  T of C in the onshore from that of offshore regions along the Kuroshio, eastern Taiwan. The relative abundance of picophytoplankton also changed due to the coastal uplift; the relative abundances of *Synechococcus* and picoeukaryotes increased toward onshore, but it decreased for *Prochlorococcus*. This phenomenon can be explained by the fact that the growth of *Synechococcus* and picoeukaryotes is more favorable in high nutrient availability environments, but the growth of *Prochlorococcus* is less susceptible to nutrient depletion but more vulnerable to higher temperatures. The results all suggest the coastal uplift supports more energy transferred to higher tropical levels, and it may play a key element in mapping the puzzle of the “Kuroshio paradox.”

## DATA AVAILABILITY STATEMENT

The datasets presented in this study can be found in online repositories. The names of the repository/repositories and accession number(s) can be found below: [doi.org/10.5061/dryad.bzkh1899p](https://doi.org/10.5061/dryad.bzkh1899p).

## REFERENCES

- Acabado, C. S., Cheng, Y.-H., Chang, M.-H., and Chen, C.-C. (2021). Vertical nitrate flux induced by Kelvin-Helmholtz billows over a seamount in the Kuroshio. *Front. Mar. Sci.* 8:680729. doi: 10.3389/fmars.2021.680729
- Agawin, N. S., Duarte, C., Agustí, S., and Vaqué, D. (2004). Effect of N:P ratios on response of Mediterranean picophytoplankton to experimental nutrient inputs. *Aquat. Microb. Ecol.* 34, 57–67. doi: 10.3354/ame034057
- Alvain, S., Moulin, C., Dandonneau, Y., and Breon, F. M. (2005). Remote sensing of phytoplankton groups in case 1 waters from global SeaWiFS imagery. *Deep-Sea Res. Part I-Oceanogr. Res. Pap.* 52, 1989–2004. doi: 10.1016/j.dsr.2005.06.015
- Buck, K. R., Chavez, F. P., and Campbell, L. (1996). Basin-wide distributions of living carbon components and the inverted trophic pyramid of the central gyre of the north Atlantic Ocean, summer 1993. *Aquat. Microb. Ecol.* 10, 283–298. doi: 10.3354/ame010283
- Buitenhuis, E. T., Li, W. K. W., Vault, D., Lomas, M. W., Landry, M. R., Partensky, F., et al. (2012). Picophytoplankton biomass distribution in the global ocean. *Earth Syst. Sci. Data* 4, 37–46. doi: 10.5194/essd-4-37-2012

## AUTHOR CONTRIBUTIONS

C-CChen contributed to designing of the research, analyzing data, and writing the manuscript. C-YL performed the research (Chl *a*, dissolved inorganic nutrients) and analyzed the data. SJ performed the research (water volume transport), analyzed the data, and wrote part of the manuscript. C-hH performed the research (picoplankton abundance) and analyzed data. C-CChung performed the research (picoplankton abundance) and analyzed the data. All authors contributed to manuscript revision and approved the submitted version.

## FUNDING

This study is part of the multidisciplinary “Plankton Ecological Processes in Subtropical-shelf Ecosystems” (PEPSE) and “The Observations of the Kuroshio Transports and their Variability” (OKTV) programs, which are supported by the Ministry of Science and Technology, Taiwan (MOST; 107-2611-M-003-001-MY3 and 110-2611-M-003-002 to C-CChen). SJ was supported by the MOST grant no. 101-2611-M-002-018-MY3, 103-2611-M-002-011, and 105-2119-M-002-042.

## ACKNOWLEDGMENTS

We are indebted to the officers and crew of the *Ocean Researcher I* for their assistance during the research cruise. This article was subsidized by National Taiwan Normal University (NTNU).

## SUPPLEMENTARY MATERIAL

The Supplementary Material for this article can be found online at: <https://www.frontiersin.org/articles/10.3389/fmars.2022.796187/full#supplementary-material>

- Calvo-Díaz, A., Díaz-Pérez, L., Suárez, L. Ñ, Morán, X. A. G., Teira, E., and Marañón, E. (2011). Decrease in the autotrophic-to-heterotrophic biomass ratio of picoplankton in oligotrophic marine waters due to bottle enclosure. *Appl. Environ. Microbiol.* 77, 5739–5746. doi: 10.1128/AEM.00066-11
- Campbell, L., Nolla, H. A., and Vault, D. (1994). The importance of *Prochlorococcus* to community structure in the central North Pacific Ocean. *Limnol. Oceanogr.* 39, 954–961. doi: 10.4319/lo.1994.39.4.0954
- Chan, Y. F., Chung, C. C., Gong, G. C., and Hsu, C. W. (2020). Spatial variation of abundant picoeukaryotes in the subtropical Kuroshio Current in winter. *Mar. Ecol.* 41:e12579. doi: 10.1111/maec.12579
- Chang, M.-H., Jan, S., Mensah, V., Andres, M., Rainville, L., Yang, Y. J., et al. (2018). Zonal migration and transport variations of the Kuroshio east of Taiwan induced by eddy impingements. *Deep-Sea Res. Part I-Oceanogr. Res. Pap.* 131, 1–15. doi: 10.1016/j.dsr.2017.11.006
- Chen, C. T. A., Liu, C. T., and Pai, S. C. (1995). Variations in oxygen, nutrient and carbonate fluxes of the Kuroshio Current. *La Mer* 33, 161–176.
- Chen, C.-C., Gong, G.-C., Chiang, K.-P., Shiah, F.-K., Chung, C.-C., and Hung, C.-C. (2021). Scaling effects of a eutrophic river plume on organic carbon consumption. *Limnol. Oceanogr.* 66, 1867–1881. doi: 10.1002/lno.11729

- Chen, C.-C., Hsu, S.-C., Jan, S., and Gong, G.-C. (2015). Episodic events imposed on the seasonal nutrient dynamics of an upwelling system off northeastern Taiwan. *J. Mar. Syst.* 141, 128–135. doi: 10.1016/j.jmarsys.2014.07.021
- Chen, C.-C., Jan, S., Kuo, T. H., and Li, S. Y. (2017). Nutrient flux and transport by the Kuroshio east of Taiwan. *J. Mar. Syst.* 167, 43–54. doi: 10.1016/j.jmarsys.2016.11.004
- Chung, C.-C., and Gong, G.-C. (2019). Attribution of the growth of a distinct population of *Synechococcus* to the coverage of lateral water on an upwelling. *Terr. Atmos. Ocean. Sci.* 30, 575–587. doi: 10.3319/tao.2018.09.26.01
- Cushman-Roisin, B. (1994). *Introduction to Geophysical Fluid Dynamics*. Hoboken, NJ: Prentice-Hall.
- Endo, H., and Suzuki, K. (2019). “Spatial variations in community structure of haptophytes across the Kuroshio front in the Tokara Strait,” in *The Kuroshio-Induced Nutrient Supply in the Shelf and Slope Region off the Southern Coast of Japan*, eds T. Nagai, H. Saito, K. Suzuki, and M. Takahashi (Hoboken, NJ: John Wiley & Sons, Inc), 207–221. doi: 10.1002/9781119428428.ch13
- Furuya, K. (1990). Subsurface chlorophyll maximum in the tropical and subtropical western Pacific Ocean: vertical profiles of phytoplankton biomass and its relationship with chlorophyll a and particulate organic carbon. *Mar. Biol.* 107, 529–539. doi: 10.1007/BF01313438
- Gong, G.-C., Wen, Y.-H., Wang, B.-W., and Liu, G.-J. (2003). Seasonal variation of chlorophyll a concentration, primary production and environmental conditions in the subtropical East China Sea. *Deep-Sea Res. II Top. Stud. Oceanogr.* 50, 1219–1236. doi: 10.1016/S0967-0645(03)00019-5
- Guo, Y. J. (1991). The Kuroshio, Part II. Primary productivity and phytoplankton. *Oceanogr. Mar. Bio. Ann. Rev.* 29, 155–189.
- Hsu, S. C., Wong, G. T. F., Gong, G. C., Shiah, F. K., Huang, Y. T., Kao, S. J., et al. (2010). Sources, solubility, and dry deposition of aerosol trace elements over the East China Sea. *Mar. Chem.* 120, 116–127. doi: 10.1016/j.marchem.2008.10.003
- Hung, C. C., and Gong, G. C. (2011). Biogeochemical responses in the Southern East China Sea after Typhoons. *Oceanography* 24, 42–51. doi: 10.5670/oceanog.2011.93
- Jan, S., Chen, C. C., Tsai, Y. L., Yang, Y. J., Wang, J., Chern, C. S., et al. (2011). Mean structure and variability of the cold dome Northeast of Taiwan. *Oceanography* 24, 100–109. doi: 10.5670/oceanog.2011.98
- Jan, S., Mensah, V., Andres, M., Chang, M.-H., and Yang, Y. J. (2017). Eddy-Kuroshio interactions: local and remote effects. *J. Geophys. Res. Oceans* 122, 9744–9764. doi: 10.1002/2017JC013476
- Jan, S., Yang, Y. J., Wang, J., Mensah, V., Kuo, T.-H., Chiou, M.-D., et al. (2015). Large variability of the Kuroshio at 23.75°N east of Taiwan. *J. Geophys. Res. Oceans* 120, 1825–1840. doi: 10.1002/2014JC010614
- Jiao, N., and Yang, Y. (2002). Ecological studies on *Prochlorococcus* in China seas. *Chinese Sci. Bull.* 47, 1243–1250. doi: 10.1360/02tb9276
- Kobari, T., Honma, T., Hasegawa, D., Yoshie, N., Tsutsumi, E., Matsuno, T., et al. (2020). Phytoplankton growth and consumption by microzooplankton stimulated by turbulent nitrate flux suggest rapid trophic transfer in the oligotrophic Kuroshio. *Biogeosciences* 17, 2441–2452. doi: 10.5194/bg-17-2441-2020
- Kodama, T., Shimizu, Y., Ichikawa, T., Hiroe, Y., Kusaka, A., Morita, H., et al. (2014). Seasonal and spatial contrast in the surface layer nutrient content around the Kuroshio along 138°E, observed between 2002 and 2013. *J. Oceanogr.* 70, 489–503. doi: 10.1007/s10872-014-0245-5
- Lai, C.-C., Wu, C.-R., Chuang, C.-Y., Tai, J.-H., Lee, K.-Y., Kuo, H.-Y., et al. (2021). Phytoplankton and bacterial responses to monsoon-driven water masses mixing in the Kuroshio off the east coast of Taiwan. *Front. Mar. Sci.* 8:707807. doi: 10.3389/fmars.2021.707807
- Lee, S., and Fuhrman, J. A. (1987). Relationship between biovolume and biomass of naturally derived marine bacterioplankton. *Appl. Environ. Microbiol.* 53, 1298–1303. doi: 10.1016/0198-0254(87)96080-8
- Levitus, S. (1982). *Climatological Atlas of the World Ocean, NOAA Professional Paper No. 13*. Silver Spring, Md: US Government Printing Office.
- Li, J., Jiang, X., Li, G., Jing, Z., Zhou, L., Ke, Z., et al. (2017). Distribution of picoplankton in the northeastern South China Sea with special reference to the effects of the Kuroshio intrusion and the associated mesoscale eddies. *Sci. Total Environ.* 589, 1–10. doi: 10.1016/j.scitotenv.2017.02.208
- Lin, F. S., Ho, P. C., Sastri, A. R., Chen, C. C., Gong, G. C., Jan, S., et al. (2020). Resource availability affects temporal variation of phytoplankton size structure in the Kuroshio east of Taiwan. *Limnol. Oceanogr.* 65, 236–246. doi: 10.1002/lno.11294
- Liu, H. B., Suzukil, K., Minami, C., Saino, T., and Watanabe, M. (2002). Picoplankton community structure in the subarctic Pacific Ocean and the Bering Sea during summer 1999. *Mar. Ecol. Prog. Ser.* 237, 1–14. doi: 10.3354/Meps237001
- Liu, H., Nolla, H. A., and Campbell, L. (1997). Prochlorococcus growth rate and contribution to primary production in the equatorial and subtropical North Pacific Ocean. *Aquat. Microb. Ecol.* 12, 39–47. doi: 10.3354/ame012039
- Liu, K., Suzuki, K., Chen, B., and Liu, H. (2020). Are temperature sensitivities of *Prochlorococcus* and *Synechococcus* impacted by nutrient availability in the subtropical northwest Pacific? *Limnol. Oceanogr.* 66, 639–651. doi: 10.1002/lno.11629
- Marañón, E., Holligan, P. M., Barciela, R., González, N., Mourinho, B., Pazó, M. J., et al. (2001). Patterns of phytoplankton size structure and productivity in contrasting open-ocean environments. *Mar. Ecol. Prog. Ser.* 216, 43–56. doi: 10.3354/meps216043
- McWilliams, J. C., Colas, F., and Molemaker, M. J. (2009). Cold filamentary intensification and oceanic surface convergence lines. *Geophys. Res. Lett.* 36:L18602. doi: 10.1029/2009GL039402
- Mensah, V., Jan, S., Andres, M., and Chang, I. H. (2020). Response of the Kuroshio east of Taiwan to mesoscale eddies and upstream variations. *J. Oceanogr.* 76, 271–288. doi: 10.1007/s10872-020-00544-8
- Mensah, V., Jan, S., Chang, M. H., and Yang, Y. J. (2015). Intraseasonal to seasonal variability of the intermediate waters along the Kuroshio path east of Taiwan. *J. Geophys. Res. Oceans* 120, 5473–5489. doi: 10.1002/2015jc010768
- Mensah, V., Jan, S., Chiou, M.-D., Kuo, T. H., and Lien, R.-C. (2014). Evolution of the Kuroshio Tropical water from the Luzon Strait to the east of Taiwan. *Deep-Sea Res. Part I-Oceanogr. Res. Pap.* 86, 68–81. doi: 10.1016/j.dsr.2014.01.005
- Morel, A., Ahn, Y.-H., Partensky, F., Vaulot, D., and Claustre, H. (1993). *Prochlorococcus* and *Synechococcus*: a comparative study of their optical properties in relation to their size and pigmentation. *J. Mar. Res.* 51, 617–649. doi: 10.1135/0022240933223963
- Mourinho-Carballido, B., Hojas, E., Cermeño, P., Chouciño, P., Fernández-Castro, B., Latasa, M., et al. (2016). Nutrient supply controls picoplankton community structure during three contrasting seasons in the northwestern Mediterranean Sea. *Mar. Ecol. Prog. Ser.* 543, 1–19. doi: 10.3354/meps11558
- Nagai, T. (2019). *The Kuroshio Current: Artery of Life*. Washington, DC: John Wiley & Sons.
- Nagai, T., Durán, G. S., Otero, D. A., Mori, Y., Yoshie, N., Ohgi, K., et al. (2019). How the Kuroshio current delivers nutrients to sunlit layers on the continental shelves with aid of near-internal waves and turbulence. *Geophys. Res. Lett.* 46, 6726–6735. doi: 10.1029/2019GL082680
- Nagai, T., Tandon, A., and Rudnick, D. L. (2006). Two-dimensional ageostrophic secondary circulation at ocean fronts due to vertical mixing and large-scale deformation. *J. Geophys. Res.* 111:C09038. doi: 10.1029/2005JC002964
- Nitani, H. (1972). “Beginning of the Kuroshio,” in *Kuroshio: Its Physical Aspects*, eds H. Stommel and K. Yoshida (Tokyo: University of Tokyo Press), 129–163.
- Olson, R. J., Chisholm, S. W., Zettler, E. R., Altabet, M. A., and Dusenberry, J. A. (1990). Spatial and temporal distributions of prochlorophyte picoplankton in the North Atlantic Ocean. *Deep-Sea Res. Part I-Oceanogr. Res. Pap.* 37, 1033–1051. doi: 10.1016/0198-0149(90)90109-9
- Parsons, T. R., Maita, Y., and Lalli, C. M. (1984). *A Manual of Chemical and Biological Methods for Seawater Analysis*. Oxford, NY: Pergamon Press.
- Raven, J. A. (1998). The twelfth tansley lecture. small is beautiful: the picophytoplankton. *Funct. Ecol.* 12, 503–513. doi: 10.1046/j.1365-2435.1998.00233.x
- Rochford, D. J. (1984). Nitrates in eastern Australian coastal waters. *Aust. J. Mar. Freshwater Res.* 35, 385–397. doi: 10.1071/MF9840385
- Roughan, M., and Middleton, J. H. (2002). A comparison of observed upwelling mechanisms off the east coast of Australia. *Cont. Shelf Res.* 22, 2551–2572. doi: 10.1016/S0278-4343(02)00101-2
- Shiah, F. K., Gong, G. C., and Chen, C. C. (2003). Seasonal and spatial variation of bacterial production in the continental shelf of the East China Sea: possible

- controlling mechanisms and potential roles in carbon cycling. *Deep-Sea Res. II Top. Stud. Oceanogr.* 50, 1295–1309. doi: 10.1016/S0967-0645(03)00024-9
- Smayda, T. J., and Reynolds, C. S. (2001). Community assembly in marine phytoplankton: application of recent models to harmful dinoflagellate blooms. *J. Plankton Res.* 23, 447–461. doi: 10.1093/plankt/23.5.447
- Sukigara, C., Suga, T., Toyama, K., and Oka, E. (2014). Biogeochemical responses associated with the passage of a cyclonic eddy based on shipboard observations in the western North Pacific. *J. Oceanogr.* 70, 435–445. doi: 10.1007/s10872-014-0244-6
- Thurnherr, A. M. (2010). A practical assessment of the errors associated with full-depth LADCP profiles obtained using teledyne RDI workhorse acoustic doppler current profilers. *J. Atmos. Ocean. Tech.* 27, 1215–1227. doi: 10.1175/2010jtecho708.1
- Visbeck, M. (2002). Deep velocity profiling using lowered acoustic doppler current profilers: bottom track and inverse solutions. *J. Atmos. Ocean. Tech.* 19, 794–807. doi: 10.1175/1520-0426(2002)019<0794:dvpu>2.0.co;2
- Wal, P. V. D., Kraay, G. W., and Meer, J. V. D. (1994). Community structure and nutritional state of phytoplankton growing in mesocosms with different initial N:P ratios studied with high performance liquid chromatography. *Sarsia* 79, 409–416. doi: 10.1080/00364827.1994.10413572
- Worden, A. Z., Follows, M. J., Giovannoni, S. J., Wilken, S., Zimmerman, A. E., and Keeling, P. J. (2015). Rethinking the marine carbon cycle: factoring in the multifarious lifestyles of microbes. *Science* 347:1257594. doi: 10.1126/science.1257594
- Wu, C.-R., Wang, Y.-L., Lin, Y.-F., Chiang, T.-L., and Wu, C.-C. (2016). Weakening of the Kuroshio intrusion into the South China Sea under the global warming hiatus. *IEEE J. Sel. Top. Appl. Earth Obs. Remote Sens.* 9, 5064–5070. doi: 10.1109/JSTARS.2016.2574941
- Wu, L. X., Cai, W. J., Zhang, L. P., Nakamura, H., Timmermann, A., Joyce, T., et al. (2012). Enhanced warming over the global subtropical western boundary currents. *Nat. Clim. Change* 2, 161–166. doi: 10.1038/Nclimate1353
- Yang, H., Lohmann, G., Wei, W., Dima, M., Ionita, M., and Liu, J. (2016). Intensification and poleward shift of subtropical western boundary currents in a warming climate. *J. Geophys. Res. Oceans* 121, 4928–4945. doi: 10.1002/2015JC011513
- Conflict of Interest:** The authors declare that the research was conducted in the absence of any commercial or financial relationships that could be construed as a potential conflict of interest.
- Publisher's Note:** All claims expressed in this article are solely those of the authors and do not necessarily represent those of their affiliated organizations, or those of the publisher, the editors and the reviewers. Any product that may be evaluated in this article, or claim that may be made by its manufacturer, is not guaranteed or endorsed by the publisher.
- Copyright © 2022 Chen, Lu, Jan, Hsieh and Chung. This is an open-access article distributed under the terms of the Creative Commons Attribution License (CC BY). The use, distribution or reproduction in other forums is permitted, provided the original author(s) and the copyright owner(s) are credited and that the original publication in this journal is cited, in accordance with accepted academic practice. No use, distribution or reproduction is permitted which does not comply with these terms.